EUROPEAN MECHANICAL SCIENCE

Research Article

e-ISSN: 2587-1110

Investigation of the effects of luster glazes on chamotte bodies

Merve Öztorun[1], **Nermin Demirkol**[2*]

[1] Kocaeli University, Institute of Social Sciences, Department of Ceramics, 41300, Türkiye
[2] Kocaeli University, Faculty of Fine Arts, Department of Ceramics, 41300, Türkiye

Abstract: Luster is a thin metallic film formed on the glaze surface through the migration and reduction of metal ions under a reducing atmosphere. This film causes optical interference, producing metallic and iridescent color effects. In this study, silver nitrate ($AgNO_3$) was used as the luster-forming agent. During reduction, silver ions migrate toward the glaze surface and are reduced to metallic silver. Glaze formulations containing $AgNO_3$ and various lead-based and alkaline metal oxides were prepared and brush-applied onto chamotte clay test tablets biscuit fired at 1000 °C. The glazed samples were first heated to 1000°C in a gas-fired raku kiln over 2 hours to ensure proper glaze maturation. After the firing process was completed, the tablets were removed with tongs when the kiln temperature dropped to 850°C through free cooling. For the reduction process, sawdust, newspaper, dried fruit, walnut, and hazelnut shells were prepared in a metal barrel, and the test tablets were placed in the metal barrel and subjected to reduction for 20 minutes. After the reduction process, samples A and D exhibited gold-brown effects on the test surfaces, while samples B and C exhibited gold-copper and iridescent rainbow effects. Microstructural analyses were performed on post-firing samples. The analyses confirmed the presence of Ag and Cu ions on the surface of samples A, B, C, and D. The chamotte body's rough and porous structure caused partial glaze absorption, reducing luster intensity; however, increased glaze thickness improved luster development, while surface roughness contributed a distinctive textural aesthetic.

Keywords: Luster Glaze; Reduction; Chamotte Clay; Silver Nitrate; Ceramics

1. Introduction

Luster glazes are a traditional type of glaze that gives ceramic surfaces an optically rich, metallic appearance. The luster technique was first applied to transparent glass by glassmakers in Egypt during the Abbasid Caliphate in the 8th century [1-3]. This technique, which originated in the Islamic world, began to appear in Spain with the first luster examples brought from North Africa. Today, although the luster is not the same as the first examples, the technique used is the same. Luster is the formation of a pearl-like film layer on the surface of the glaze by the reduction of metal compounds [4-6]. It is known that the glass matrix layer formed on the surface of the glaze, with silver and copper ions embedded in this layer, creates the metallic reflection on the surface [7,8]. Luster formation is divided into two types according to the atmosphere inside the kiln: reduction and oxidation. Among these, the glaze-internal luster technique, which belongs to the reduction type, is the focus of this study. In this technique, metal salts and oxides are added to the glaze, and the reduction process is applied during the cooling phase after firing the glaze in an oxidizing atmosphere. The success of the luster effect depends not only on the glaze formulation and firing conditions but also on the interaction between the glaze and the ceramic body to which it is applied [9,10].

Luster has been in existence since the 8th century and continues to attract great interest today for its aesthetic appeal. From that period to the present day, luster glaze recipes using the overglaze luster technique have been predominant. What distinguishes this study from others is that it creates new recipes using the luster glaze technique instead of the overglaze luster technique. Another difference is the use of chamotte body instead of white body, demonstrating the applicability of luster glazes to different bodies. It shows that even simple glaze formulations prepared using transparent glazes containing metal oxides and a single metal salt can yield excellent results when luster glaze techniques are used in new artistic discoveries.

*Corresponding author:
Email: nermin.demirkol@kocaeli.edu.tr

Cite this article as:
Öztorun, M., Demirkol, N. (2025). Investigation of the effects of luster glazes on chamotte bodies. *European Mechanical Science*, 9(4): 320-327. https://doi.org/10.26701/ems.1837641

History dates:
Received: 07.12.2025, *Revision Request*: 18.12.2025, *Last Revision Received*: 20.12.2025, *Accepted*: 23.12.2025

© Author(s) 2025. This work is distributed under https://creativecommons.org/licenses/by/4.0/

In this study, various metal oxides and a metal salt, silver nitrate ($AgNO_3$), were added in specific proportions to two different glaze formulations: one alkali-based and the other lead-based. These glaze mixtures were applied to chamotte clay bodies and then subjected to reduction firing. The behavior of the lustrous glazes on the chamotte clay body was examined. The microstructural features, layer thickness, integrity, and glaze–body interface were comprehensively evaluated using Scanning Electron Microscopy (SEM) and Energy Dispersive X-ray Spectroscopy (EDS) techniques. Metallic crystalline phases on the glaze surface were additionally characterized by X-ray Diffraction (XRD) analyses.

2. Materials and Methods

2.1. Glaze Recipe Calculations and Preparation of the Glazes

Two different recipes, boron-alkali and lead-based, were created using Herman Seger's recipe calculation methods. The recipes exhibit bright, transparent properties at 1000oC. The raw materials used for the created recipes are shown in Table 1 and Table 2. The raw materials were obtained in milled form from the "Refsan" company. Glaze preparation and firing processes were carried out at the Ceramic Technology Laboratory in the Faculty of Fine Arts at Kocaeli University. The raw materials used in the study were weighed on a precision scale according to the ratios specified in Table 1 and Table 2, and the glaze recipes were prepared by milling them in a ball mill with water for 30 minutes.

Table1. Glaze Recipe 1

Raw Materials	(wt. %)
Ulexite	20
Borax	20
K- Felspar	20
N- Felspar	15
Zinc Oxide	2.5
Zircon	2.5
Dolomite	5
Kaoline	10
Quartz	5

Raw Materials	(wt. %)
Lead tetroxide	20
Borax	42
N- Felspar	26
Quartz	12

2.2. Firing Process of the Samples

In this study, test tablets were fabricated by placing the plastic, chamotte-rich body into plaster molds, followed by densification under a controlled mechanical compaction method. Firstly, test tablets were first subjected to a bisque firing at 1000 °C in an oxidizing atmosphere in order to remove physically bound water and to stabilize the ceramic bodies prior to glazing. Following the bisque stage, two glaze formulations developed within the scope of the study were applied onto the surfaces of the bisque-fired tablets using a controlled brush application technique to ensure uniform coating thickness. Subsequently, the glazed samples were fired once again under oxidizing conditions to complete the glaze maturation process.

Based on the initial base glaze composition, 20 g of each liquid glaze sample was weighed, and predetermined amounts of various metal oxides together with silver nitrate ($AgNO_3$) were incorporated to produce four distinct glaze formulations. These formulations are presented in Table 3 as Sample A, Sample B, Sample C, and Sample D.

Following the addition of the metal oxides and $AgNO_3$, the mixtures were wet-milled in a ball mill for 20 minutes to ensure adequate dispersion, reduction of particle clustering, and the formation of a homogeneous glaze suspension suitable for application [11-13]. The milling process was conducted under controlled conditions to maintain consistent slurry characteristics and to optimize the reactivity of the added materials during subsequent firing stages [14].

Table 3. Details of Luster Glaze Recipes

Sample Code	Metal Oxides (wt. %)	Metal Salt (wt. %)
Sample A	1R + %3 MnO	%2 $AgNO_3$
Sample B	1R + %10 CuO %5 Fe_2O_3 %1 $Cu(NO_3)_2$	%2 $AgNO_3$
Sample C	1R + %3 Fe_2O_3 %1 CuO	%2 $AgNO_3$
Sample D	2R + %1 MnO	%2 $AgNO_3$

Following the milling process in the ball mill, the glaze suspensions were evaluated in terms of their rheological properties and particle size distribution to ensure suitability for application. The prepared glaze formulations were then applied onto the surfaces of the chamotte body test tablets, which had previously undergone bisque firing at 1000°C, using a controlled brush application technique to achieve a uniform coating thickness. After application, the glazed tablets were allowed to dry under ambient conditions to stabilize the surface moisture and promote homogeneous glaze distribution. Following the completion of the preparatory processes, the glazed test tablets were prepared for the final firing stage, which was carried out under a reduc-

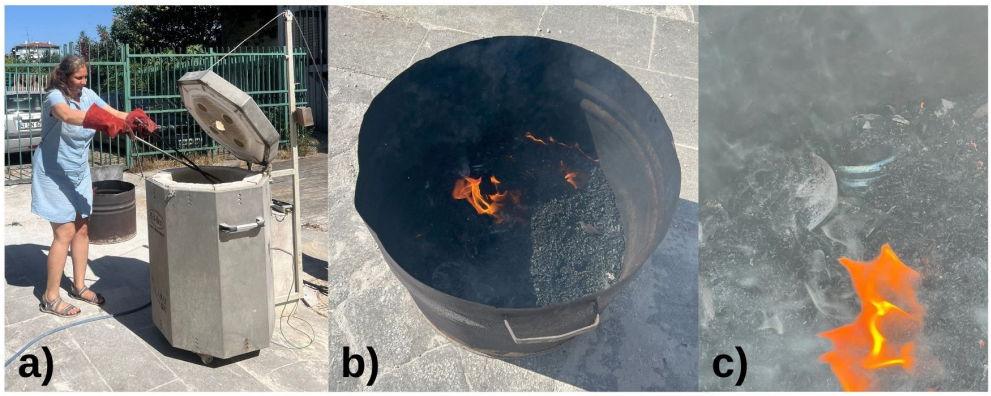


Figure 1. Samples Coated with Luster Glaze, (a) Firing in a Raku Kiln, (b) Reduction Stage, (c) Detailed View of the Reduction Stage

ing kiln atmosphere to promote the formation of the characteristic luster layer.

Following the glazing stage, the samples were placed in the gas-fired kiln and ignited using an LPG burner. The firing schedule was adjusted so that the kiln reached 1000 °C within approximately 2 hours. After reaching peak temperature, the samples were soaked at 1000 °C fora 10 minutes. Subsequently, the gas supply to the kiln was cut off, allowing the system to cool naturally to 850 °C. Once the kiln temperature decreased to 850 °C, the samples were removed from the chamber, as shown in Figure 1(a), and immediately transferred into the metal reduction container illustrated in Figure 1(b). The reduction atmosphere was generated using a mixture of organic materials, including wood shavings, newspaper, walnut shells, hazelnut shells, and onion skins. The condition of the samples during the reduction process is presented in Figure 1(c)

2.3. Characterization of Luster Glazed Samples

Cross-sections of Samples with luster glaze that have undergone the reduction process samples were examined using scanning electron microscopy (SEM) and energy-dispersive X-ray spectroscopy (EDX) analyses to investigate microstructures. The analysis was performed using a JEOL JSM-6060VL scanning electron microscope. For SEM imaging, the samples were coated with gold for 90 seconds. This method ensures that the samples are conductive, allowing for better microstructure analysis. EDS analysis were also performed on SEM samples 15.0 kV acceleration with a 35.0° angle and at 100X magnification SEM and EDS analysis were performed.

XRD analyses were performed to determine the phase analyses of reduction-processed luster-glazed samples. All diffraction measurements were carried out using a Rigaku Ultima III X-ray diffractometer operating at 40 kV and 40 mA. Diffraction patterns were collected using CuKα radiation (λ = 0.154 nm) over a 2θ scanning range of 5–80° at a scanning speed of 2°/min.

3. Results

3.1. Luster Glaze Firing Results

The oxidative firing results of Recipe 1 (alkali-based) and Recipe 2 (lead-based) are presented in Figure 2, where both glaze formulations exhibit transparent and glossy surface characteristics [15].

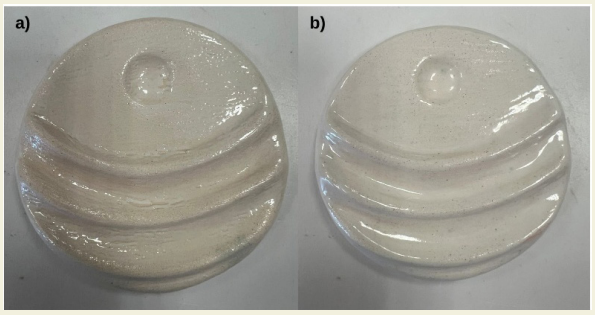


Figure 2. Image of (a) Recipe 1 and (b) Recipe 2 fired in an oxidizing atmosphere at 1000°C

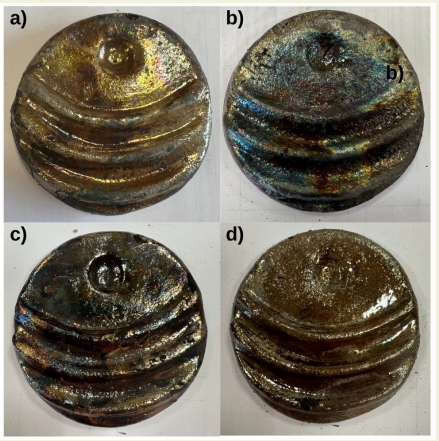


Figure 3. Images of Luster Glazed (a) Sample A, (b) Sample B, (c) Sample C and (d) Sample D After Reduction Firing

3 wt% MnO and 2 wt% $AgNO_3$ were added for Sample A, prepared from Recipe 1. As shown in Figure 3(a), brown tonalities originating from MnO are visible in the background, while the reduction of silver ions from $AgNO_3$ results in a pronounced golden luster effect. This observation is consistent with previous studies demonstrating that noble-metal nanoparticle formation under reducing atmospheres governs luster colour development [5, 16].

Sample B was produced by incorporating 10 wt% CuO, 5 wt% FeO, 1 wt% $Cu(NO_3)_2$, and $AgNO_3$ into Recipe 1. As shown in Figure 3b, a combined appearance of copper-red luster (derived from copper compounds) and golden luster (originating from silver) was obtained. This result aligns with studies reporting that copper and silver salts may co-form metallic nanocrystals during reduction firing [17, 18].

Sample C was prepared by adding 3 wt% Fe_2O_3, 1 wt% CuO, and 2 wt% $AgNO_3$ to Recipe 1. In Figure 3c, red-brown hues originating from Fe_2O_3 and CuO are accompanied by gold and iridescent (rainbow-like) luster effects produced by $AgNO_3$. Such complex colouration is in accordance with literature indicating that multi-metal nanoparticle systems can yield richer luster appearances in ceramic glazes [18, 20].

1 wt% MnO and 2 wt% $AgNO_3$ were added for Sample D, produced from the lead-bearing Recipe 2. As shown in Figure 3d, the luster response resembles that of Sample A, which can be attributed to the use of MnO in both formulations, albeit in different proportions. However, due to the lead content, Recipe 2 maintains full transparency, whereas Recipe 1 exhibits a slight loss of transparency after reduction firing. This behaviour is associated with the presence of opacifying oxides such as ZrO_2 and SnO_2 in Recipe 1, which tend to induce partial opacification under reducing conditions an effect also reported in the literature [5].

As a result, Sample A contains an alkali and boron-containing glaze, while sample D contains a lead-containing glaze. In contrast, the use of MnO as a colorant in varying proportions in both samples produced similar results. In both samples, a golden luster effect from $AgNO_3$ was observed on a brown background originating from MnO. Samples B and C were colored with the same metal oxides in different proportions to the alkali boron-containing glazes. However, unlike $AgNO_3$, the metal salt $Cu(NO_3)_2$ was used in sample B. This resulted in a more pronounced rainbow effect in sample B. It has been demonstrated that different luster effects can be achieved by using the same metal oxides in different ratios.

3.2. Microstructure Analyses (SEM and EDS)

SEM cross-sectional imaging revealed an irregular glaze–body interface between the applied glaze and the chamotte ceramic substrate, while the glaze surfaces nonetheless exhibited pronounced and aesthetically successful metallic/luster effects. Although similar luster phenomena were observed for both lead-containing and alkaline glazes when the same metallic additives were used, distinct microstructural and visual differences were also evident (Fig 4). In addition to the metallic luster, textured surface morphologies contributed to additional aesthetic variations.

Cross-sections were examined by scanning electron microscopy (SEM) and localized chemical analyses were performed using energy-dispersive X-ray spectroscopy (EDS). Glaze layer thicknesses were measured from the SEM section images, and intraglass porosity related to melt behaviour was observed. The interlayer formed at the chamotte–glaze contact was discontinuous and heterogeneous, which we attribute to uneven glaze penetration into the porous chamotte body [15]

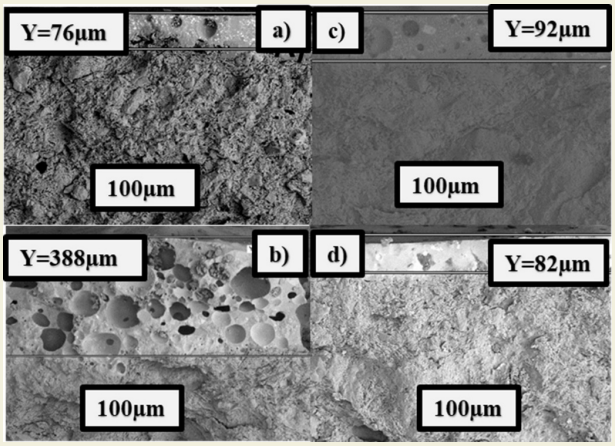


Figure 4. Glaze Thickness of the Samples-SEM Sectional Images Sample (a), (b), (c) and (d).

Glaze thicknesses from cross-sectional images are shown in Figure 4. The glaze thicknesses of samples A, B, C, and D were measured as 76µm, 92µm, 388µm, and 82µm, respectively, as seen in Figures 4(a), 4(b), 4(c), and 4(d).

Leaded glazes showed greater melt fluidity and consequently lower glaze porosity compared with alkali glazes, where lower meltability correlated with larger and more frequent pores [19]. EDS point analysis detected silver (Ag) and copper (Cu) signals in the glazed layers; Ag was predominantly concentrated near the glaze surface, consistent with surface segregation of noble metal species during reduction cooling, whereas Cu-rich particles appeared more irregularly distributed in subsurface regions [21]. The presence of a thin metallic film consistent with a luster layer was confirmed by SEM imaging and EDS elemental mapping.

The presence of silver (Ag) and copper (Cu) has been confirmed on the surface of the lustrous glaze. Ag par-

ticles are more concentrated on the surface, while Cu distribution shows deeper penetration towards the intermediate layer. Metallic phases form more distinct concentration areas on the white body, while the distribution on the chamotte body is more irregular. Due to its porous structure, chamotte clay absorbs the glaze into the body, so the glaze application is thicker.

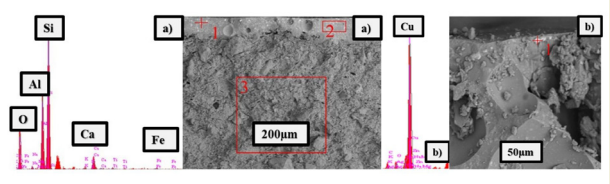


Figure 5. SEM Cross Sectional Images of (a) Sample A and (b) Sample B.

Point EDS analyses were performed on cross-sections of samples taken from the glaze layer. The (+2) analysis performed on the SEM image with a 200 µm scale bar of sample A revealed a distinct chamotte structure beneath the glaze layer (Fig 5 (a)). The predominance of Si, Al, O, and Ca elements in the EDS analysis indicates that the glaze has a typical silicate-glass phase structure. The detection of low levels of Fe indicates naturally occurring iron oxide from the raw material. The distinct pore structure within the body (region 3) is consistent with the microstructure seen in porous ceramics containing chamotte [22]. Furthermore, the microstructure and bubble structures on the glaze surface are indicative of gas release occurring in the glass phase during firing.

In the SEM image with a 50 µm scale bar cross-sectional image of sample B, copper-rich regional accumulations are observed within the glaze layer. Strong Cu peaks in the EDS analysis indicate that Cu^{2+} → Cu^{0} or Cu^{+} conversion occurred in a reducing atmosphere. This is entirely consistent with the formation mechanism of luster and copper-red glazes [23,24]. In the SEM image, irregular metallic Cu nanoparticles embedded within the glassy phase were observed in the upper region of the glaze (Fig 5 (b)). The glaze-substrate intifaca was observed to have a more heterogeneous structure. The accumulation of copper towards the surface has formed a metallic film layer due to the effects of reduction conditions [25].

The first (+1) point analysis performed on the SEM image with a 50 µm scale bar of sample C analyzed the nano particle appearing as a rectangle. The EDS point analysis (+1) indicates that Fe is the dominant element (Fig 6(c)). This indicates the presence of dense FeO or Fe_2O_3 phases within the glaze. Glazes containing Fe are known to tend toward darker and more metallic tones due to the $Fe^{3+} \rightarrow Fe^{2+}$ conversion in a reducing atmosphere [26] The SEM image shows numerous spherical voids on the surface and Fe and Cu particles embedded in the glassy phase. The detection of the Cu peak in-

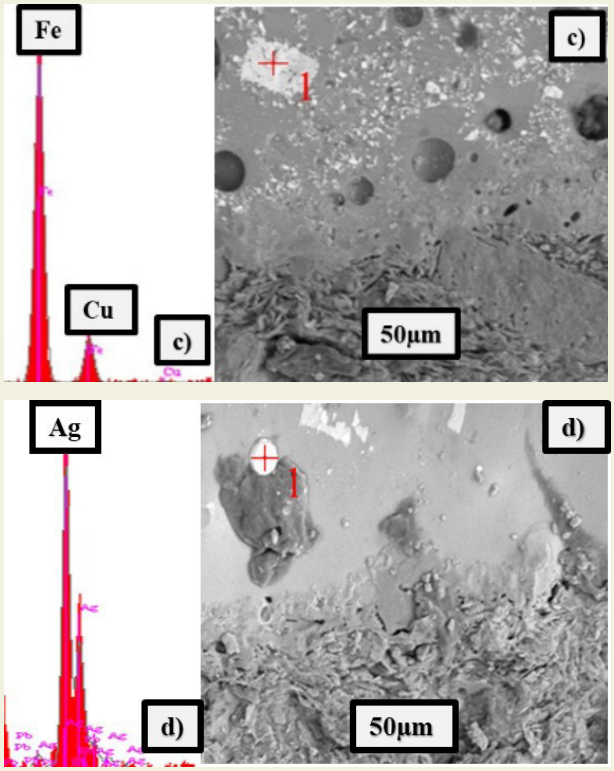


Figure 6. SEM Cross Sectional Images of (c) Sample C and (d)Sample D

dicates that a low amount of Cu oxide was used in the glaze composition and that it was reduced together with Fe to form microstructured metallic formations.

In the SEM image with a 50 µm scale bar cross-section image of sample D point EDS analysis yielded high Ag peaks (+1) (Fig 6(d)). This indicates that Ag^{+} ions in the glaze were reduced to metallic Ag particles in a reducing atmosphere and that the mechanism of brightness formation is effective [27].

In the SEM image, dense metallic silver islands in the upper part of the glaze layer, nano/micro-sized Ag particles dispersed in the glassy phase, and a distinct interface between the porous chamotte body and the glaze are visible. Furthermore, since sample D is a lead-containing glaze, it exhibited better surface melting compared to alkaline glaze recipes. This is because lead lowers the melting point of the glaze compared to alkalis. This microstructure closely resembles the structure of traditional Islamic luster glazes. In particular, the concentration of Ag nanoparticles in the regions close to the surface is the most critical indicator of the optical film behavior that creates the brightness effect.

The ionic exchange between Na+ or K+ and Cu+ and Ag+ in the solution occurs during firing in a reducing atmosphere. During this reduction phase, nanocrystals of metallic copper and metallic silver are formed. The typical sizes of the nanocrystals are 15 to 20 nm for copper Cu and 5 to 20 nm for silver Ag. The composition of

the glaze is very important for the development of the luster film layer. [28]

3.3. XRD Analysis

The XRD patterns presented in Figure 7 reveal an amorphous glassy matrix accompanied by characteristic reflections corresponding to metallic silver (Ag) and copper (Cu) crystals, zircon silicate ($ZrSiO_4$), and silica-based phases.

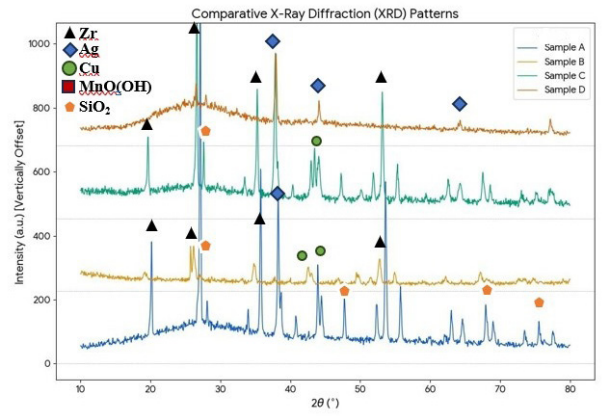


Figure 7. XRD Analysis of Samples A B, C and D

The most intense diffraction peak is associated with zircon silicate for Sample A. Additionally, reflections corresponding to kyanite (Al_2SiO_5) and metallic Ag are observed. Previous studies have demonstrated that zircon silicate does not contribute to the formation of metallic luster, as the surface luster effect is primarily attributed to Ag nanoparticles precipitated under reducing conditions [29]. Thus, the luster observed in Sample A is considered to arise predominantly from metallic Ag.

The XRD pattern of Sample B shows relatively low-intensity peaks associated with keatite, silica, and zircon silicate phases compared with the other samples. Peaks corresponding to Cu and Ag phases are also present, indicating the reduction of both metals to crystalline forms during firing. The simultaneous presence of Cu and Ag nanoparticles is known to enhance the chromatic intensity of luster effects [30]

In Sample C, the most intense peak again corresponds to zircon silicate; however, the Ag peak intensity is the highest among all samples. Similarly, Cu reflections exhibit strong peak intensities, confirming the presence of substantial Ag–Cu metallic aggregates on the surface. The close relationship between the concentration of Ag and Cu nanoparticles and the intensity of the luster effect has been well documented. These findings are consistent with the pronounced golden and copper-red metallic sheen observed in Figure 3.

The XRD pattern of Sample D displays the most intense peak for metallic Ag. In addition, quartz (SiO_2) and barysilite ($Pb_8Si_6O_{21}$) a phase commonly found in lead-bearing glaze systems were identified. The MnO component in the recipe was detected as manganite (MnO(OH)).

Overall, zircon silicate reflections dominate the surface XRD analysis; however, previous research indicates that this phase does not contribute significantly to luster formation. Instead, the luster effect arises from Ag and Cu nanoparticles that develop under reducing firing conditions. The present study corroborates these findings by demonstrating that the luster intensity in all samples is directly associated with the crystalline metallic phases detected in the XRD patterns.

4. Conclusions

This study demonstrated that the microstructural and aesthetic outcomes of luster formation in metal-bearing glazes are strongly governed by both the chemical composition of the glaze and the firing atmosphere. SEM–EDS analyses revealed that the four experimental samples exhibited markedly different behaviors under reducing conditions, primarily due to their distinct elemental compositions. In glazes containing Cu, Fe, and Ag, the reduction of transition-metal ions was clearly observed, accompanied by the formation of metallic aggregates within the glassy matrix. These metallic clusters contributed directly to the characteristic luster effects obtained on the surfaces.

This study demonstrates that luster color and intensity can be effectively controlled by adjusting the type and proportion of metal salts and oxides in different glaze systems, with $AgNO_3$ producing golden luster tones, while CuO and copper nitrate enhance rainbow-like optical effects.

The interface between the chamotte body and the glaze proved to be heterogeneous and irregular in all samples. This was attributed to the porous nature of the chamotte body, which promoted uneven glaze absorption and resulted in discontinuous interfacial layers. Lead-bearing glazes showed superior melt fluidity and consequently lower porosity, while alkaline glazes exhibited larger and more frequent pores due to reduced meltability.

In addition to microstructural differences, notable aesthetic variations emerged. The textured surface of the chamotte body imparted a rough morphology that interacted with the glaze layer, enhancing the visual depth of the luster. It was also observed that increasing glaze thickness amplified the intensity of the luster effect, likely due to higher concentrations of reduced metal species and more efficient light reflection from metallic surface films. Silver-containing glazes produced golden and iridescent luster tones, whereas copper-bearing glazes yielded blue, violet, purple, and reddish reflections consistent with established reduction-based color

mechanisms.

Overall, the findings confirm that the reducing atmosphere plays a critical role in driving metal-ion reduction, metallic particle formation, and the development of luster layers in ceramic glazes. The combined influence of glaze composition, melt behavior, body porosity, and glaze thickness determines both the microstructural features and the final artistic appearance. These results provide valuable insight into the controlled production of luster surfaces and highlight the importance of optimizing glaze formulation and firing parameters to achieve targeted visual effects in ceramic art and technology.

Acknowledgement

In this study, I would like to express my deepest gratitude to the Scientific Research Projects Directorate of Kocaeli University for their financial support for the project with code SYL-2024-3781. I would like to express my deepest gratitude to Sakarya University,

Faculty of Engineering, Department of Metallurgy and Materials Engineering for SEM, EDS, and XRD analysis.

Research Ethics

Ethical approval not required.

Artificial Intelligence Use

I hereby declare that artificial intelligence (ChatGPT, Gemini) was used in this study to verify the references.

Author Contributions

Conceptualization: [Merve Öztorun, Nermin Demirkol], Methodology: [Merve Öztorun, Nermin Demirkol] , Formal Analysis: [Merve Öztorun, Nermin Demirkol], Investigation: [Merve Öztorun], Resources: [Merve Öztorun, Nermin Demirkol], Data Curation: [Merve Öztorun], Writing - Original Draft Preparation: [Merve Öztorun, Nermin Demirkol], Writing - Review & Editing: [Merve Öztorun, Nermin Demirkol], Visualization: [Merve Öztorun, Nermin Demirkol], Supervision: [Nermin Demirkol], Project Administration: [Nermin Demirkol], Funding Acquisition: [Merve Öztorun, Nermin Demirkol]

Competing Interests

The author(s) declare that there are no competing interests.

Research Funding

University of Kocaeli Scientific Research Department (Project ID: SYL-2024-3781).

Data Availability

Not applicable.

Peer-review

Externally peer-reviewed.

Orcid

Merve Öztorun https://orcid.org/0009-0002-6416-1826
Nermin Demirkol https://orcid.org/0000-0001-9088-023X

References

[1] Pradell T. et al. (2008). The invention of lustre: Iraq 9th and 10th centuries AD. Journal of Archaeological Science, 35(5), 1201–1215. https://doi.org/10.1016/j.jas.2007.08.016

[2] Carboni S. (2001). Glass From Islamic Lands. Thames & Hudson.London, UK.

[3] Yoleri, H., & Çiftçi, F. (2025). Luster paste applications on glass surfaces. Yedi Journal of Art, Desing& Science. (34), 1-12. https://doi.org/10.17484/yedi.1635314

[4] Caiger-Smith, A. (1991). Lustre Pottery: Technique, Tradition and Innovation in Islam and the Western World New. Amsterdam Books. New York, USA.

[5] Ağıl, A.A., & Karasu, B. (2019). A general look over the characterisation of lustre glazes. El-Cezerî Journal of Science and Engineering, 6(1), 51–79. https://doi.org/10.31202/ecjse.454149

[6] Roque J. et al. (2008). Analytical study of lustre ceramic decorations. Phase Transitions, 81, 267–282. https://doi.org/10.1080/01411590701514441

[8] Pradell T. et al. (2008). The invention of luster. Journal of Archaeological Science, 35, 1201–1215. https://doi.org/10.1016/j.jas.2007.08.016

[10] Daly, G. (2012). Lustre Handbook. A&C Black. London, UK.

[9] Mouhebati H., & Kösler A.T. (2019). Golden Lustre On Ceramics With Spraying Method. Dumlupınar University Journal Of Social Sciences, Special Issue, 81-90.http://dergipark.gov.tr/dpusbe

[11] Kingery, W. D., Bowen, H. K., & Uhlmann, D. R. (1976). Introduction to Ceramics. New York, USA (Wiley).

[12] Bohren, C.F., & Huffman, D.R. (1998). Absorption and Scattering of Light by Small Particles. Germany (Wiley).

[13] Reed J.S. (1995). Principles of Ceramics Processing. New York, USA (Wiley).

[14] Hamer, F., & Hamer, J. (2004). The Potter's Dictionary. A&C Black. London, UK.

[15] Öztorun, M., & Demirkol, N.. Investigation of the effects of luster glazes on chamotte

[16] Çalışkan Güneş, P. (2019). Luster from a reduced environment. İdil , 8(54), 283–288. https://doi.org/10.7816/idil-08-54-20

[17] İmer, C., Günay, E., & Öveçoğlu, M. L. (2016). Effects of firing temperatures and compositions on the formation of nano particles in lustre layers on a lead-alkali glaze. Ceramics International, 42(15), 17222–17228. https://doi.org/10.1016/j.ceramint.2016.08.014Get rights and content

[18] Kılınç Mirdalı, N., Daday, M., & Daday, M. T. (2019). Development and characterization of low temperature metallic glazes in Na_2O-B_2O_3-SiO_2 (NBS) system. Ceramics International, 45(17), 21661–21667. https://doi.org/10.1016/j.ceramint.2019.07.164

[19] Sintering-Based In-Situ Synthesis and Characterization by TEM of Noble Metal Nanoparticles for Ceramic Glaze Color Control. (2021).

Nanomaterials, 11(8), 2103. https://doi.org/10.3390/nano11082103

[20] Lohner, T., Agócs, E., Petrik, P., Zolnai, Z., Szilágyi, E., Kovács, I., Szőkefalvi-Nagy, Z., Tóth, L., Illés, L., & Bársony, I. (2014). Spectroellipsometric and ion beam analytical studies on a glazed ceramic object with metallic lustre decoration. Applied Physics A, 115, 1389–1398. https://doi.org/10.1007/s00339-014-8375-8

[21] Korean Ceramic Society (2023). Silver nitrate gold luster glaze. Korean Journal of Ceramic Science & Technology, 20(3). https://doi.org/10.22991/ksca.2023.20.3.7

[22] Barsoum, M.W. (2003). Fundamentals of Ceramics. Taylor & Francis. New York, USA

[23] Zanella L. et al. (2015). Characterization of metallic nanoparticles in historical lustre. Applied Surface Science, 351, 669–677. https://doi.org/10.1016/j.apsusc.2015.03.033

[24] Pradell, T., Pavlov, R. S., Gutiérrez, P. C., Climent-Font, A., & Molera, J. (2012). Composition, nanostructure, and optical properties of silver and silver-copper lusters. Journal of Applied Physics, 112(5), 054307/1-12. https://doi.org/10.1063/1.4749790

[25] Pradell, T., Molera, J., Bayés, C., & Roura, P. (2006). Luster decoration of ceramics: Mechanisms of metallic luster formation. Applied Physics A, 83, 203–208. https://doi.org/10.1007/s00339-006-3508-1

[26] Kingery, W. D., Bowen, H. K., & Uhlmann, D. R. (1976). Introduction to ceramics (2nd ed.). New York, USA(Wiley).

[27] J. Molera, M. Mesquida, J. Perez-Arantegui, T. Pradell, and M. Vendrell, "Luster recipes from a medieval workshop in Paterna," Archaeometry 43(4), 455–460 (2001). https://doi.org/10.1111/1475-4754.00028

[28] Pradell, T., Molera, J., Bayés, C., & Roura, P. (2006). Luster decoration of ceramics: Mechanisms of metallic luster formation. Applied Physics A, 83(2), 203–208. https://doi.org/10.1007/s00339-006-3508-1

[29] Tite, M. S., Pradell, T., & Shortland, A. (2008). The technology of lustre and tin-based glazes. Journal of Archaeological Science, 35, 596–626. https://doi.org/10.1016/j.jas.2007.09.012

[30] Malins, J. P., & Tonge, K. H. (1999). Reduction processes in the formation of lustre glazed ceramics. Thermochimica Acta, 340–341, 395–405. https://doi.org/0040-6031/99/$